Supplementary Material for "Setting Boundaries with Memory: Generation of Topological Boundary States in Floquet-Induced Synthetic Crystals"

Yuval Baum[1] and Gil Refael[1]

[1] *Institute of Quantum Information and Matter, California Institute of Technology, Pasadena, California 91125, USA*

LOCAL-IN TIME FORMALISM AND NUMERICAL EVOLUTION

In this section we derive a local-in-time formalism for the dynamics of Eq. (8) in the main text. This formalism was used to produce the numerical time evolution results shown in the main text. Our starting point is:

$$\mathrm{i}\partial_t\psi_x(t) = \sum_{x'}\mathcal{H}_{x-x'}(t)\psi_{x'}(t) + \int_0^T u_{x-x'}(\tau)\psi_{x'}(t-\tau)\frac{\mathrm{d}\tau}{T}. \tag{S1}$$

Since $u(\tau)$ is defined only in the range $\tau\in[0,T]$, we may write it as $u_{x-x'}(\tau)=\sum_n u_{n,x-x'}e^{\mathrm{i}n\omega\tau}$, where $\omega=2\pi/T$. Next, we define the following quantity:

$$\phi_{n,x'}(t) = \frac{1}{T}\int_0^T e^{\mathrm{i}n\omega\tau}\psi_{x'}(t-\tau)\mathrm{d}\tau. \tag{S2}$$

Hence, Eq. (8) can be written as follows:

$$\mathrm{i}\partial_t\psi_x(t) = \sum_{x'}\mathcal{H}_{x-x'}(t)\psi_{x'}(t) + \sum_n u_{n,x-x'}\phi_{n,x'}(t). \tag{S3}$$

The time derivative of Eq. (S2) fulfills:

$$\begin{aligned}\mathrm{i}\partial_t\phi_{n,x}(t) &= -\int_0^T e^{\mathrm{i}n\omega\tau}\partial_\tau\psi_x(t-\tau)\frac{\mathrm{i}\mathrm{d}\tau}{T}\\ &= -\frac{\mathrm{i}}{T}\Big[\psi(x,t-T)-\psi(x,t)\Big] - n\omega\phi_{n,x}(t)\\ &= \frac{1}{\mathrm{i}T}\Big[e^{\mathrm{i}\eta T}-1\Big]\psi_x(t) - n\omega\phi_{n,x}(t),\end{aligned} \tag{S4}$$

where in the last step we assumed that ψ has a Floquet form. Overall, we replaced an integro-differential equation, Eq. (8), by a set of local-in-time differential equations:

$$\begin{aligned}\mathrm{i}\partial_t\psi_x(t) &= \sum_{x'}\mathcal{H}_{x-x'}(t)\psi_{x'}(t) + \sum_n u_{n,x-x'}\phi_{n,x'}(t)\\ \mathrm{i}\partial_t\phi_{n,x}(t) &= \frac{1}{\mathrm{i}T}\Big[e^{\mathrm{i}\eta T}-1\Big]\psi_x(t) - n\omega\phi_{n,x}(t)\end{aligned} \tag{S5}$$

Notice that unlike the set of equations in Eq. (12) and Eq. (13) in the main text, the above equations define a non-hermitian system (non-unitary dynamics) of the field ψ and the fields ϕ_n. The above system may be written as follows:

$$\mathrm{i}\partial_t\Psi(x,t) = M(x-x',t)\Psi(x',t), \tag{S6}$$

where $\Psi(x,t)=\Big(\psi(x,t)\ \ldots\ \phi_{-1}(x,t)\ \ \phi_0(x,t)\ \ \phi_1(x,t)\ \ldots\Big)^T$, and M is the non-hermitian Hamiltonian of the system.

A knowledge of the field ψ and the fields ϕ_n at $t=0$, determines completely the dynamics, i.e.,

$$\Psi(x,t) = \mathcal{T}\exp\Big(-\mathrm{i}\int_0^t M(x-x',t')\mathrm{d}t'\Big)\Psi(x',0). \tag{S7}$$

Considering a wave-packet with x and n as coordinates. At any time, the center of the wave-packet, both in x and n spaces, may be evaluated:

$$\begin{aligned}\langle x(t)\rangle &= \int \mathrm{d}x'\, x|\psi(x,t)|^2,\\ \langle n(t)\rangle &= \sum n|\phi_n(x,t)|^2,\end{aligned} \tag{S8}$$

For the Hamiltonian and the memory kernel of the $1+1$D case in the main text, we now consider four different initial states. The first two states are localized in

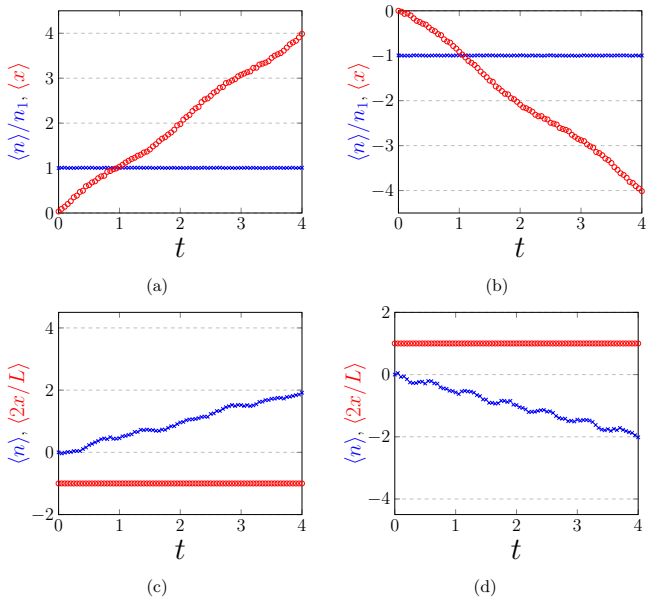

FIG. S1. The center of a wave-packet in real space, $\langle x(t)\rangle$, (red) and in photon space, $\langle n(t)\rangle$, (blue) as a function of time for the four different initial states: (a) $\psi_{1,+}$ (b) $\psi_{1,-}$ (c) $\psi_{2,+}$ (d) $\psi_{2,-}$.

the middle of the chain with a well defined number of photons, where the topological transitions occur:

$$\Psi_{1,\pm}(x,0) = \begin{cases} \psi(x,0) = \phi_{n=\pm n_1}(x,0) = e^{-(x/x_0)^2} \begin{pmatrix} 1 \\ 0 \end{pmatrix} \\ \phi_{n\neq\pm n_1}(x,0) = 0. \end{cases} \tag{S9}$$

The other two states are localized on the right/left edge of the chain with no photons:

$$\Psi_{2,\pm}(x,0) = \begin{cases} \psi(x,0) = \phi_{n=0}(x,0) = \delta(x \pm L/2) \begin{pmatrix} 1 \\ 0 \end{pmatrix} \\ \phi_{n\neq 0}(x,0) = 0. \end{cases} \tag{S10}$$

In all four cases we used Eq. (S7) to determine the time evolution and calculate $\langle x(t)\rangle$ and $\langle n(t)\rangle$. In all cases we avoided the corners in the $x-n$ space where the numerics is not reliable because of the sharp edges. In the following, we set v_0 and ω to unity and therefore $T = 2\pi$. We find the evolution of the initial states using Eq. (S7) for short time segments $dt = 10^{-4}T$. See Fig. S1. Evidently, the numerical results agree qualitatively with the analytical analysis. For the first case (initial state in the bulk with $n = n_1$), the variance $\langle n^2\rangle$ remains zero due to the fact that states with different number of photons are gapped. The variance $\langle x^2\rangle$ remains unchanged (up to a numerical error) which is a manifestation of the linear dispersion relation ($\epsilon = k$). For the second case (initial state on the edge with $n = 0$), the variance $\langle x^2\rangle$ remains zero due to the lack of bulk states with low number of photons. The variance $\langle n^2\rangle$ fluctuates. We believe that this is a numerical artifact, which we can not get rid of, and not a true feature.

PSEUDO-SPIN FIELD COUPLED TO A CHIRAL FIELD

In the main text we discussed the case of a (pseudo) spin field coupled to a chiral field and showed that a memory kernel of the desired form may be achieved. In Eq. (15) in the main text we found that the Fourier components of the memory kernel $u(t)$ may be expressed in terms of the Fourier components of the coupling $\lambda(x)$ as follows:

$$u_n = \sum_{m\neq n} \frac{2\mathrm{Re}(\lambda_m \lambda_n^\dagger)}{2\pi(n-m)}. \tag{S11}$$

if $\lambda_n = \text{const}$ for $|n| < n_0$ and zero otherwise, the resultant u_n is approximately linear for $|n| \ll n_0$. For large n_0 this is sufficient to screen the electric field in an extensive region. These λ_l correspond to the function

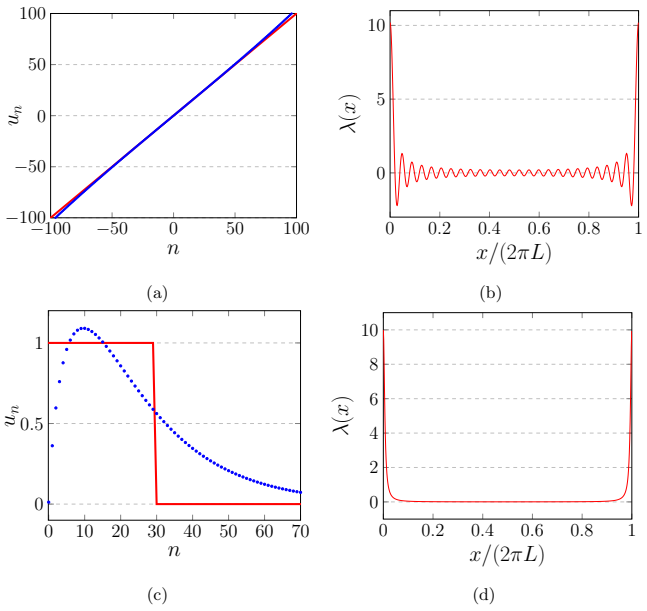

FIG. S2. For $\lambda_n = \text{const} \times \Theta(|n| - 250)$ (a) is the resultant u_n (blue) vs. a perfect linear potential (red) and (b) is the corresponding $\lambda(x)$. (c,d) same as (a,b) only for $\lambda_n = \exp(-|n|/25)$.

shown in Fig. S2b, which is oscillatory with wave number n_0/L. The resultant u_n and the corresponding $\lambda(x)$ are depicted in Fig. S2a and b. An exact rectangular function is not accessible, but a smoother version of a rectangular function can be generated. For example, for $\lambda_n \sim \exp(-|n|/n_1)$, a smooth crossover between a topological and trivial region occurs. The resultant u_n and the corresponding $\lambda(x)$ are depicted in Fig. S2c and d.

In the main text we consider the coupling of a spin field to a chiral 1D field. However, it is possible to get a similar effect with a non-chiral field. Assume a standard non-chiral wire (quadratic dispersion) in which the chemical potential is located high above the bottom of the band. The excitations in that case can be treated as two decoupled (left and right) chiral fields. In that case the corresponding memory kernel has the required form and its Fourier components are given by:

$$u_n = \sum_{m\neq n} \frac{\mathrm{Re}(\lambda_{R,m}\lambda_{R,n}^\dagger + \lambda_{L,-m}\lambda_{L,-n}^\dagger)}{\pi(n-m)}, \tag{S12}$$

where $\lambda_{R/L}$ refer to the coupling to the right/left moving modes. This formula may lead to similar memory kernels as in the chiral case. For clean systems, deviations from the above formula arise due to curvature effects. However, as long as the chemical potential is the largest energy scale in the problem, these deviations are small.